

Geometrically-parameterized Circuit Models of Printed Circuit Board Traces Inclusive of Antenna Coupling

*Original*

Geometrically-parameterized Circuit Models of Printed Circuit Board Traces Inclusive of Antenna Coupling / Triverio, Piero; GRIVET TALOCIA, Stefano; Bandinu, Michelangelo; Canavero, Flavio. - In: IEEE TRANSACTIONS ON ELECTROMAGNETIC COMPATIBILITY. - ISSN 0018-9375. - STAMPA. - 52:2(2010), pp. 471-478. [10.1109/TEMC.2010.2043256]

*Availability:*

This version is available at: 11583/2365848 since:

*Publisher:*

IEEE

*Published*

DOI:10.1109/TEMC.2010.2043256

*Terms of use:*

This article is made available under terms and conditions as specified in the corresponding bibliographic description in the repository

*Publisher copyright*

(Article begins on next page)

# Geometrically Parameterized Circuit Models of Printed Circuit Board Traces Inclusive of Antenna Coupling

Piero Triverio, *Member, IEEE*, Stefano Grivet-Talocia, *Senior Member, IEEE*, Michelangelo Bandinu, and Flavio G. Canavero, *Fellow, IEEE*

**Abstract**—This paper presents a systematic methodology for the characterization of mutual couplings between antennas and printed circuit board (PCB) traces in modern mobile devices. The main approach is based on the assumption that the interfering fields produced by the antennas are not perturbed significantly by the PCB traces. The one-way coupling can thus be computed using the theory of field-excited transmission lines. The incident field patterns excited by each antenna are computed via a single preliminary full-wave analysis. We adopt a generalized scattering formulation for the electromagnetic system. Some ports define the terminals of the PCB traces, the other “electromagnetic” ports correspond to the antennas feed points. The main achievement of this paper is a parameterization scheme for this generalized scattering form in terms of the trace-routing path. This parameterization further approximates the frequency dependence of each response in terms of rational functions, enabling the direct synthesis of path-dependent macromodels in an SPICE environment. Fast optimization, what-if, and sensitivity analyses can thus be performed directly via transient SPICE runs, possibly including realistic (transistor-level or behavioral) models for driver and receiver circuits.

**Index Terms**—Antenna coupling, electromagnetic interference (EMI), interpolation, parametric modeling, rational approximation, transmission-line modeling.

## I. INTRODUCTION

THIS paper addresses the immunity characterization of modern mobile devices and cell phones to self-generated electromagnetic (EM) disturbances. Both technological advances and market expectations are leading to an aggressive integration of multiple functionalities in very compact volumes. Digital circuits for data processing and storage must coexist in close proximity to the analog and radio-frequency blocks responsible for wireless communications. Good isolation between different functional blocks is, therefore, mandatory.

The general analysis of such structures requires a careful characterization of all significant EM interactions. This can be accomplished to some extent using state-of-the-art full-wave solvers. However, general applicability of this approach is severely limited by two main factors. First, the extreme

complexity of real-world structures, in terms of fine geometrical details, inevitably leads to a very large number of unknowns in the discretization of the EM fields. For instance, printed circuit board (PCB) traces carrying high-speed digital signals have widths that are much smaller than the area where they are routed in. They are subject to interfering fields radiated by the device antennas, and these fields should be computed by embedding the device in some free space model with suitable absorbing boundary conditions. Even adaptive meshing leads to prohibitive complexity if all details are considered in a single run.

The second limiting factor is due to the large number of degrees of freedom that are still not finalized during early stages of a design flow. An example is the routing path of PCB traces. EM characterization must be repeated several times during the design cycle, to accommodate for what-if analyses, sensitivity, and optimization studies. Therefore, a fast parameterization of the device parts as a function of the relevant design parameters is highly desirable, together with a fast methodology to estimate EM couplings.

This paper presents a fast methodology for the characterization of coupling between device antennas and PCB traces. The main assumption is that the PCB traces do not load the radiating antennas significantly. Therefore, the near fields produced by each antenna are evaluated using a single preliminary full-wave analysis performed with the unpopulated board. Then, the well-established theory of field-excited transmission lines is applied to evaluate the EM coupling from the antenna into an arbitrarily routed PCB trace. This characterization is described in a generalized scattering form. Some standard ports correspond to the electrical terminals of the PCB trace, whereas the remaining “electromagnetic” ports correspond to the antenna feed points. The aforementioned process is documented in [1].

The procedure that is highlighted in [2] further processes the aforementioned data by a rational curve-fitting algorithm. This technique, usually denoted as macromodeling, allows the synthesis of a lumped equivalent circuit using standard methods. Such equivalents are readily converted into SPICE netlists, thus enabling transient analysis for signal integrity and EM interference (EMI) assessments including the effects of nonlinear terminations such as digital drivers and receivers.

In this paper, we further extend this idea, by presenting a parameterization approach for the time-domain macromodels of the traces (including the EMI effects), in terms of their routing path. Two main directions are investigated, depending on the

Manuscript received September 30, 2009. Current version published May 19, 2010.

The authors are with the Department of Electronics, Politecnico di Torino, Torino 10129, Italy (e-mail: piero.triverio@polito.it; stefano.grivet@polito.it; michelangelo.bandinu@polito.it; flavio.canavero@polito.it).

Color versions of one or more of the figures in this paper are available online at <http://ieeexplore.ieee.org>.

Digital Object Identifier 10.1109/TEM.2010.2043256

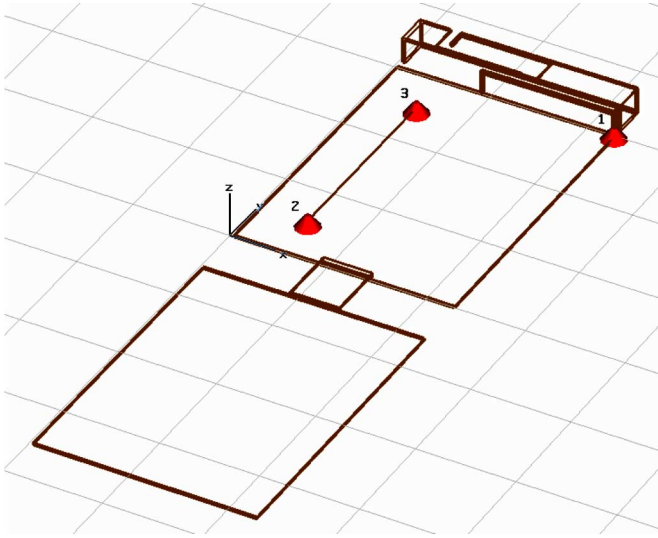


Fig. 1. Outline of a mobile phone and definition of the electrical ports.

type of parameterization that is adopted, one based on a variable-length, while the second based on a discrete grid of fixed-length short line segments. In both cases, the main result consists of two parameterized SPICE netlists, one for horizontal and one for vertical segments. Any complex routing path can be reduced by cascading in a global SPICE deck different instances of these subcircuits for different parameter values. Therefore, the generation of the fully coupled netlist for an arbitrarily routed path is achieved via simple function evaluations (this can be performed directly in a SPICE environment), without requiring regeneration of the macromodel at each step.

We remark that the approach presented is mainly intended for preliminary (prelayout) analysis, since not all effects are considered in the electromagnetic analysis. In particular, the board is assumed not to be populated by the several lumped devices, components, and packages that will be present in the final design. However, very fast results may be obtained, including fast optimization and sensitivity analyses based on time-domain metrics, providing useful guidelines for placement and routing under EMI constraints.

## II. OBJECTIVES

This section describes the problem at hand and sets the main objectives of this paper. Theoretical developments and numerical results will follow in Section III and V, respectively. The problem is stated below with reference to a specific mobile device, the clamshell phone outlined in Fig. 1. As can be noticed, only the gross features of the phone are considered in this analysis. The most important features are the phone antenna, the power-ground planes of the two PCBs in the two phone parts, and the metallic hinge that connects them. All metal parts are made of copper (conductivity  $\sigma = 5.8 \times 10^7$  S/m). The size of each ground plane is 45 mm  $\times$  60 mm  $\times$  0.5 mm. The relative permittivity of the PCB dielectric (thickness 0.06 mm) is  $\epsilon_r = 4.9$ , with a loss tangent of 0.025 at 1 GHz.

For illustration purposes, we restrict our analysis to a two-layer board, although the methodology is general and can be applied to an arbitrary number of layers. A single microstrip (width 0.1 mm and thickness 0.03 mm) is arbitrarily routed on the top layer. There are three ports where signals can be applied to the electromagnetic system. The feed of the antenna is considered as a lumped port, in the following labeled as port 1. This will be regarded as the “electromagnetic” port where the source of the interfering fields is located. The terminations of the trace will be denoted as ports 2 and 3 with coordinates  $(x_2, y_2)$  and  $(x_3, y_3)$ , respectively, taking values in the following ranges:

$$x_2, x_3 \in [\underline{x}, \bar{x}] \quad (1)$$

$$y_2, y_3 \in [\underline{y}, \bar{y}]. \quad (2)$$

The system will be described as a  $3 \times 3$  multiport element, characterized by its scattering matrix. The structure and the parameterization of this matrix follows from various assumptions, detailed in the following.

The height of the microstrip trace is quite small compared to the other geometrical dimensions (ground planes and antenna). Therefore, the location of the trace on the ground plane has a minimal influence on the antenna radiation properties, and it can be safely assumed that the scattering matrix entry  $S_{11}(j\omega)$  does not depend on the coordinates of the trace end points, as proved in [2]. For the same reason, the antenna return loss  $S_{11}(j\omega)$  is not affected if the trace is removed completely from the PCB. This is one of the main enabling factors for the proposed approach, since the incident fields due to the radiating antenna can be computed using a simplified geometry of the device, with all PCB traces removed.

Due to the various geometrical sizes involved in this problem, it can be safely assumed that the antenna-to-trace coupling coefficients  $S_{21}(j\omega)$  and  $S_{31}(j\omega)$  will be quite small with respect to all other  $S_{ik}$  terms. The results in [1] and [2] confirm that these couplings are indeed smaller than  $-40$  dB uniformly over the bandwidth of interest, that for the proposed example will extend from dc up to 4 GHz. For this reason, we consider the antenna-to-trace coupling to be one-way only, and we neglect the higher order interactions. In other terms, the coupling coefficients will be treated as a first-order perturbation to the solution of the trace in absence of interfering fields. Therefore, we set

$$S_{12}(j\omega) = S_{13}(j\omega) = 0. \quad (3)$$

Of course, if the converse problem were considered of assessing the amount of energy that is transferred to the radiated fields due to a digital signal along the trace, the reciprocity theorem would be applied, and the above trace-to-antenna coupling coefficients could be obtained by symmetry.

Following the aforementioned considerations, the insertion and return loss elements  $S_{ik}(j\omega)$   $i, k = 2, 3$  of the unexcited (straight) trace do not depend on the full set of coordinates of the end points but only on the line length  $\mathcal{L} = \sqrt{(x_2 - x_3)^2 + (y_2 - y_3)^2}$ . The parameterization of the  $S_{21}(j\omega)$  and  $S_{31}(j\omega)$  coupling coefficients depends instead on the complete set of parameters  $\lambda = \{x_2, y_2, x_3, y_3\}$ . Two main approaches will be described in Section IV in order to simplify

the problem and reduce this set of parameters. Both approaches will share the same model form

$$\begin{bmatrix} S_{11}(j\omega) & 0 & 0 \\ S_{21}(j\omega; \lambda) & S_{22}(j\omega; \mathcal{L}) & S_{23}(j\omega; \mathcal{L}) \\ S_{31}(j\omega; \lambda) & S_{32}(j\omega; \mathcal{L}) & S_{33}(j\omega; \mathcal{L}) \end{bmatrix} \quad (4)$$

via suitable redefinition of the parameter set  $\lambda$ .

### III. FIELD COUPLING COEFFICIENTS

In this section, we consider a straight line trace segment and we illustrate how the generalized scattering matrix elements of the coupled antenna-trace system are computed. The proposed approach is based on the representation of the PCB trace as a field-excited transmission line, whose electrical variables satisfy the nonhomogeneous Telegraphers' equations [3]

$$\frac{d}{d\nu} V(\nu, j\omega) + Z(j\omega)I(\nu, j\omega) = V_F(\nu, j\omega) \quad (5)$$

$$\frac{d}{d\nu} I(\nu, j\omega) + Y(j\omega)V(\nu, j\omega) = I_F(\nu, j\omega) \quad (6)$$

where  $\nu$  is the longitudinal coordinate along the trace in a local coordinate system,  $V(\nu, j\omega)$  and  $I(\nu, j\omega)$  are frequency-domain voltage and current along the line, and  $Z(j\omega)$  and  $Y(j\omega)$  are the per-unit-length transverse impedance and admittance. These parameters are easily computed using a 2-D field solver. We adopt here a method-of-moments (MoM) technique based on [4] and [5], respectively.

The forcing terms  $V_F(\nu, j\omega)$ ,  $I_F(\nu, j\omega)$  represent distributed sources along the line and are due to the interfering electromagnetic field surrounding the line. Following [6], we can express these sources as

$$V_F(\nu, j\omega) = -\frac{d}{d\nu} \int_a^b \underline{\mathcal{E}}_t^i(j\omega) d\underline{l} + \mathcal{E}_\nu^i(j\omega)|_b - \mathcal{E}_\nu^i(j\omega)|_a \quad (7)$$

$$I_F(\nu, j\omega) = -Y(j\omega) \int_a^b \underline{\mathcal{E}}_t^i(j\omega) d\underline{l} \quad (8)$$

where  $a, b$  are two points on the PCB reference (ground) plane and on the trace, respectively. The *incident* electric field  $\mathcal{E}^i(j\omega)$  is defined as the externally excited field (in the present case by the radiating phone antenna) in the presence of the return (ground) conductor, with the trace removed. Subscripts  $\nu$  and  $t$  denote the longitudinal and transverse components of the field, always with respect to the line routing path. Formulas (7) and (8) are preferred here with respect to other solutions, since no information on the magnetic field is required.

The incident electric field of distributed sources  $V_F(\nu, j\omega)$ ,  $I_F(\nu, j\omega)$  needs to be known along the line routing path and is generated by means of a single full-wave simulation by exciting the antenna feed with a unit power source with some prescribed internal impedance  $R_0$ . In all our numerical tests, we used a transient full-wave solver [7], since a single run produces a broadband representation of all fields of interest. We remark that the mesh settings in this simulation need not to be very aggressive, since the spatial variation of the fields is smooth and no small-scale geometrical features are present [1].

Once the distributed sources are available, the coupling coefficients  $S_{21}(j\omega)$  and  $S_{31}(j\omega)$  are readily computed using standard transmission-line theory. Telegraphers' equations are solved as illustrated in [3] in order to compute the non-homogeneous chain matrix representation of the line

$$\begin{bmatrix} V_2(j\omega) \\ I_2(j\omega) \end{bmatrix} = \begin{bmatrix} \Phi_{22}(j\omega) & \Phi_{23}(j\omega) \\ \Phi_{32}(j\omega) & \Phi_{33}(j\omega) \end{bmatrix} \begin{bmatrix} V_3(j\omega) \\ I_3(j\omega) \end{bmatrix} + \begin{bmatrix} V_{FT}(j\omega) \\ I_{FT}(j\omega) \end{bmatrix}. \quad (9)$$

The scattering matrix elements  $S_{21}(j\omega)$  and  $S_{31}(j\omega)$  are readily obtained by terminating the line at both ends with the selected reference impedance  $R_0$  and by solving the resulting linear system [3]. The samples of the  $3 \times 3$  scattering matrix (4) will be referred, henceforth, as "original" or "reference" data.

### IV. PARAMETRIC CIRCUIT EXTRACTION

Once the scattering parameters of the antenna-PCB system are available, they must be cast in a form compatible with time-domain circuit simulators, in order to allow for the inclusion of realistic nonlinear loads at the trace ports. As shown in [2], this can be achieved by fitting the frequency samples (4) with a rational transfer function

$$S_{ik}(j\omega) \simeq \sum_n \frac{Q_n^{ik}}{j\omega - p_n^{ik}} + Q_\infty^{ik} \quad (10)$$

for the desired parameters values, using standard algorithms such as vector fitting [8]. Since every rational transfer function is the response of a lumped electrical circuit, (10) can be readily transformed to an equivalent circuit or to a set of differential equations for later time-domain analysis.

The aforementioned procedure is valid only for a fixed geometry configuration. As illustrated in [2], every time the trace geometry is changed, both the scattering matrix (4) and the equivalent circuit have to be recomputed from the field map before the transient simulation can be launched. This processing step is particularly undesirable for those analyses that require repeated simulation runs with variable system parameters, like routing optimization under EMI constraints. Being embedded in the optimization loop, this processing will have to be repeated at every optimization step, thus increasing the overall computation time. Moreover, this approach limits the model portability, since the coupled antenna-PCB model of [2] can be provided to a user only if bundled with the computational routines and with the potentially large field map data.

The root for these limitations is the restricted validity of (10), that holds only for a single trace geometry. These difficulties are removed in the following by using a *parametric* macromodeling algorithm. All coefficients (poles and residues) in (10) will be parameterized as functions of the trace geometrical parameters  $\lambda$ . In this way, an equivalent circuit for an arbitrary trace segment will be available on-the-fly with a simple evaluation of a closed-form multivariate expression for the desired value of trace parameters  $\lambda$ .

We first review in Section IV-A some background material on parametric macromodeling. Then, we present in Section IV-B and C two general methodologies for applying this para-



metric approach to the antenna–trace coupling modeling and simulation.

### A. Parametric Macromodeling

Parametric macromodeling algorithms allow for the computation of rational models that retain, in symbolic form, the dependency on some parameters of interest. This representation is obtained via an identification process starting from a set of tabulated frequency responses of the system corresponding to several combinations of frequency and parameters within the desired bandwidth and range.

The parametric macromodeling problem has received much attention in the recent literature. Parameterization schemes are available via entire-domain [9]–[11] or subdomain [12], [13] expansions. In some formulations, poles are kept fixed and only residues are parameterized [13], [14]. In other formulations, both poles and residues are parameterized [9]–[12] leading to more accurate and physically consistent parametric models. Some formulations allow preservation of stability at the cost of higher model complexity [13], and only experimental studies on passivity enforcement have been published [13]. Some other approaches lead to more compact models, with no a priori guarantee of stability [12], which must be checked and possibly enforced as a postprocessing step [12].

Among these algorithms, we adopt the technique proposed in [10] because it guarantees the highest interpolation accuracy and supports poles parameterization. If we denote the whole  $3 \times 3$  scattering matrix as  $\mathbf{S}(j\omega; \boldsymbol{\lambda})$ , the parametric model is represented as a ratio of two parametric rational functions in pole-residue form

$$\mathbf{S}(j\omega; \boldsymbol{\lambda}) \simeq \frac{\sum_{n=1}^{\bar{n}} \frac{\mathbf{R}_n(\boldsymbol{\lambda})}{j\omega - a_n} + \mathbf{R}_0(\boldsymbol{\lambda})}{\sum_{n=1}^{\bar{n}} \frac{r_n(\boldsymbol{\lambda})}{j\omega - a_n} + r_0(\boldsymbol{\lambda})} \quad (11)$$

with fixed “dummy” poles  $\{a_n\}$  and parameterized residues in both numerator and denominator  $\mathbf{R}_n(\boldsymbol{\lambda})$  and  $r_n(\boldsymbol{\lambda})$ . These terms are expressed as multivariate polynomials in the elements of  $\boldsymbol{\lambda}$ . If  $\boldsymbol{\lambda}$  has two elements  $\lambda_1$  and  $\lambda_2$ , for example, the coefficients of (11) will read

$$\mathbf{R}_n(\boldsymbol{\lambda}) = \sum_{m_1=1}^{\bar{m}_1} \sum_{m_2=1}^{\bar{m}_2} \mathbf{R}_{nm_1m_2} T_{m_1}(\lambda_1) T_{m_2}(\lambda_2) \quad (12)$$

$$r_n(\boldsymbol{\lambda}) = \sum_{m_1=1}^{\bar{m}_1} \sum_{m_2=1}^{\bar{m}_2} r_{nm_1m_2} T_{m_1}(\lambda_1) T_{m_2}(\lambda_2) \quad (13)$$

where  $T_m(x)$  denotes the Chebychev polynomial of order  $m$ . The Chebychev basis  $\{T_m(x)\}$  is here preferred to the standard polynomial basis  $\{x^m\}$  because it improves the accuracy of the model fitting algorithm [10], thanks to the well-known numerical properties of Chebychev polynomials [15]. The model order  $\bar{n}$  and the parameterization degrees  $\bar{m}_1, \bar{m}_2$  depend on the modeling bandwidth and on the system characteristics. They can be selected using either heuristic rules or iterative refinement procedures [16]. We note that (11) is somehow different from (10). As detailed in [9] and [10], a direct parameterization of (10) is

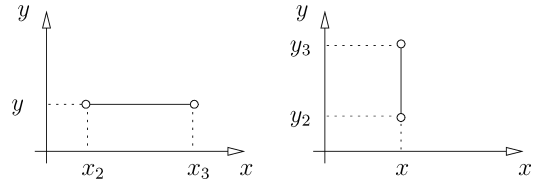


Fig. 2. (Left) Horizontal and (right) vertical traces considered in Section IV-B.

ill-conditioned due to the high variability of the model poles in the parameter space. Expression (11) parameterizes the poles (the zeros of denominator) implicitly, with improved numerical robustness. Conversion to an equivalent circuit is straightforward [12].

The identification of the coefficients of (11) is performed using a generalization of the classical Sanathanan–Koerner (SK) iteration [17], a method that is widely used in system identification because of its robustness. Even though the complexity of the algorithm in [9] and [10] is quite moderate, a direct identification of a four-variate model for  $\mathbf{S}(j\omega; \boldsymbol{\lambda})$  is a computationally intensive task. We, therefore, present two simpler approaches that are able to deliver parametric models for the antenna–PCB coupling problem with reduced computational effort.

### B. Length-Dependent Parameterization

We restrict our attention to a trace with arbitrary Manhattan routing ( $90^\circ$  bends only). In this case, only two parametric models are necessary, one for horizontal (east–west) segments and the other for vertical (north–south) segments. We detail the horizontal case, since the vertical case follows the same rules with obvious modifications.

We consider the horizontal trace depicted in the left panel of Fig. 2. Port 2 and port 3 are defined by the coordinates  $(x_2, y)$  and  $(x_3, y)$ , respectively. Therefore, only three free parameters are necessary. The model structure is the same as in (4), with  $\boldsymbol{\lambda} = \{x_2, x_3, y\}$  and  $\mathcal{L} = x_3 - x_2$ , with the three parameters spanning the ranges

$$x_2, x_3 \in [\underline{x}, \bar{x}] \quad (14a)$$

$$y \in [\underline{y}, \bar{y}] \quad (14b)$$

subject to the constraint  $x_3 > x_2$ .

Identification of the model coefficients is performed by applying a parametric SK iteration to a set of tabulated scattering responses computed over a uniform grid in the parameter space (14). However, since not all scattering elements depend on all three parameters  $x_2, x_3, y$ , we build the model in separate parts. First,  $S_{11}$  is modeled using standard vector fitting, since it does not depend on any parameter. A three-parameter model is computed for  $S_{21}$  and  $S_{31}$ , respectively. Finally, a single-parameter model ( $\mathcal{L}$ ) is computed for  $S_{ik}$   $i, k = 2, 3$ .

The main advantage of this approach is that the number of model instances required for the representation of a complex path is equal to the number of straight segments forming the path. However, as will be shown in Section V, there may be some stability issues due to the variable length.

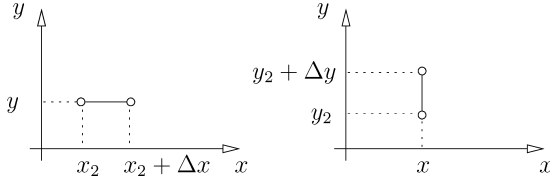


Fig. 3. Elementary trace segments of the approach given in Section IV-C. (Left) Horizontal and (right) vertical case.

### C. Fixed-Length Parameterization

In order to overcome the difficulties related to the variable trace length, we devise an alternative approach that only requires modeling of line segments of constant length. The two trace segments in Fig. 3 are the two elementary blocks of this second modeling strategy. Length is fixed, being  $\Delta x$  for the horizontal segment and  $\Delta y$  for the vertical segment. Segments are parameterized only by the coordinates of their bottom-left endpoint, calling for the definition  $\lambda = \{x_2, y_2\}$ . These two coordinates can span continuously the entire PCB area  $[\underline{x}, \bar{x}] \times [\underline{y}, \bar{y}]$  available for routing.

Model identification follows the same guidelines described above for the variable-length parameterization. Only one parameterized horizontal and one parameterized vertical model are needed. A complete model for a trace with a complex Manhattan routing path can be realized by cascading several instances of the two elementary models with different values of  $(x_2, y_2)$ . The only restriction of this second strategy is on the length of each straight path segment, that has to be a multiple of  $\Delta x$  or  $\Delta y$ , depending on its orientation. The choice of  $\Delta x$  and  $\Delta y$  results from a compromise: while smaller values provide more flexibility in the choice of the segments length, larger values lead to a more compact model. Apart from this tradeoff, the approach of this section offers a better guarantee of global model stability and results in less complexity, since the parameter space is only 2-D. We finally remark that, with the same procedure, additional elementary models can be added to support segments with arbitrary orientation (e.g.,  $45^\circ$  and  $135^\circ$  oriented traces) or paths with more complex shape like meander lines.

## V. NUMERICAL RESULTS

The two modeling strategies have been applied to the clamshell phone presented in Section II, with the microstrip routed inside the rectangle  $[\underline{x}, \bar{x}] \times [\underline{y}, \bar{y}]$  of the upper PCB ( $\underline{x} = 10$  mm,  $\bar{x} = 40$  mm,  $\underline{y} = 10.5$  mm,  $\bar{y} = 50.5$  mm). The antenna-PCB scattering parameters were computed from 0 up to 4 GHz for all possible combinations of the following parameters values:

$$x_2, x_3 \in \{10, 13.75, 17.5, 21.25, \dots, 40\} \text{ mm} \quad (15a)$$

$$y_2, y_3 \in \{10.5, 15.5, 20.5, 25.5, \dots, 50.5\} \text{ mm} \quad (15b)$$

corresponding to a uniform  $9 \times 9$  grid of points in the routing area. As standard practice in the identification of parametric models [18], part of these responses (one third) have been excluded from the fitting procedure, and reserved for a final self-validation of model accuracy.

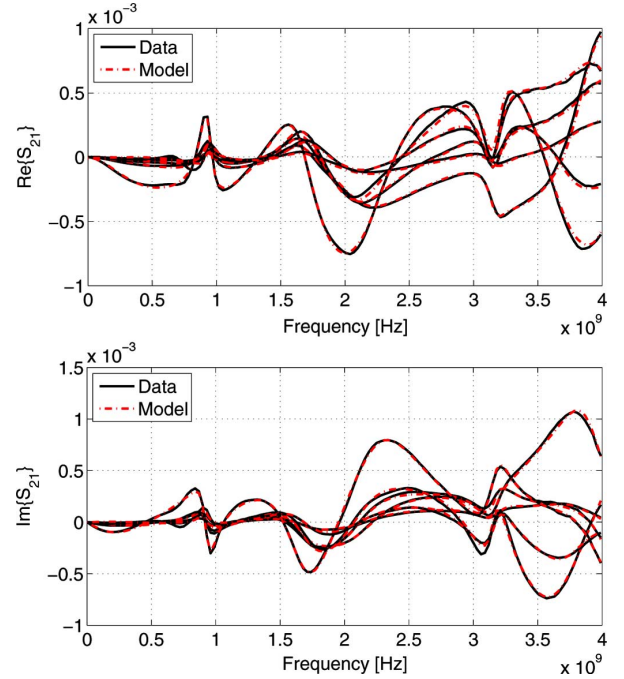


Fig. 4. Response  $S_{21}(x_1, x_2, y)$  of the parametric model for the horizontal trace of Section V-A compared with the raw scattering parameter. For plot readability, only the curves for the following parameter values are displayed:  $\lambda = \{13.75, 21.25, 40.5\}$ ,  $\{17.5, 28.75, 25.5\}$ ,  $\{28.75, 32.5, 30.5\}$ ,  $\{21.25, 36.25, 10.5\}$ ,  $\{10, 40, 35.5\}$ ,  $\{32.5, 40, 15.5\}$  mm.

### A. Modeling Results for Length-Dependent Parameterization

Figs. 4 and 5 show some responses of the parametric trace model computed with the approach of Section IV-B, compared with the reference scattering data. For the horizontal case, the model has order 18 for  $S_{11}$ , 16 for  $S_{21}$ , 20 for  $S_{31}$ , and 6 for the other coefficients. For the vertical case, orders are the same except for  $S_{21}$ , having order 18. The parameterization degree is 2 for all parameters, both at the numerator and denominator. Accuracy is quite good, as shown in the figures, where only minor discrepancies can be observed. In fact, the maximum error on validation data turned out to be  $4.7 \times 10^{-3}$  for the horizontal trace and  $4.3 \times 10^{-3}$  for the vertical case, detected in both cases on the  $S_{32}$  coefficient.

While fine for a frequency domain analysis, these models cannot be used in time-domain simulations, as some poles were found in the unstable half plane for some values of the trace length. Stability of models with parametric length is a quite challenging problem. In fact, a large number of poles is needed to accurately fit the system response for large length values. However, when the length is small, some of these poles may be redundant and their estimation may become ill-conditioned. As a result, they may fall in the unstable half plane. Even though some parametric modeling techniques with guaranteed stability are available [13], these methods have difficulties in fitting parametric systems with variable length, because of the unrealistic assumption of parameter-independent poles. Finally, algorithms for modeling transmission lines with variable length [14] are not applicable here because they do not allow one to account for the antenna-trace coupling. This example, that shows the

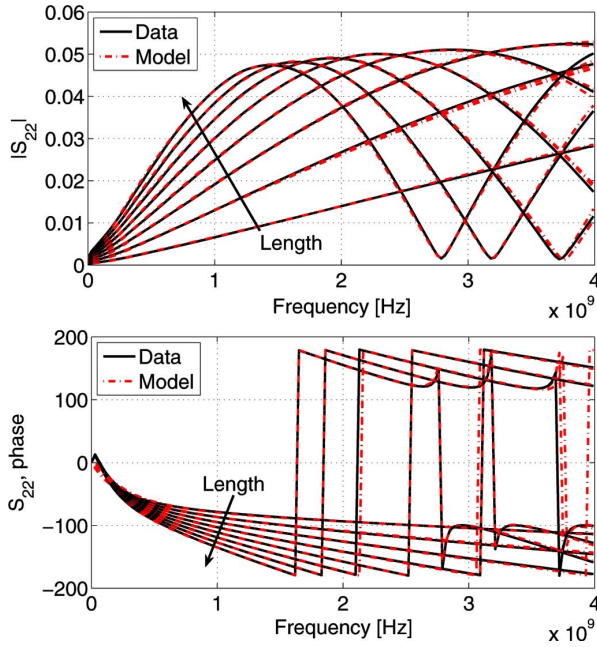


Fig. 5.  $S_{22}$  response of the parametric model of the horizontal trace described in Section V-A as a function of the trace length  $\mathcal{L}$ , plotted versus the original scattering data.

importance of the stability problem for parametric models with parameterized poles, motivated the development of the second approach of Section IV-C.

### B. Modeling Results for Fixed-Length Parameterization

The fixed-length parameterization scheme of Section IV-C has been applied to the cellphone dataset leading to the excellent results shown in Figs. 6 and 7, where the  $S_{31}$  antenna-to-microstrip coupling coefficient is depicted for the horizontal and vertical case, respectively, together with the original S-parameters. The adopted grid (15) leads to the elementary segments lengths  $\Delta x = 3.75$  mm and  $\Delta y = 5$  mm. In the horizontal case, we used a model of order 16 for  $S_{21}$  and  $S_{31}$ , order 18 for  $S_{11}$ , and order 4 for the other coefficients. For the vertical case we used the same settings, except for  $S_{21}$ , that was modeled with order 20. In both cases, model coefficients have been parameterized with a fourth order multivariate polynomial for the numerator. No parameterization has been required for the denominator coefficients, because of the fixed trace length. The worst case modeling error is  $2.5 \times 10^{-3}$  in both cases, found on the  $S_{11}$  parameter. Compared with the variable-length modeling approach, we obtained a more accurate model, thanks to the lower complexity of the parametric models to be identified. In addition, the fixed-length model is stable, and so suitable for transient simulations.

### C. Validation Example

We now validate the approach presented with respect to previous solutions published in [1] and [2]. For the geometry of Fig. 8, we derived an equivalent circuit model using the approach of Section IV-C and the method of [1] and [2], that

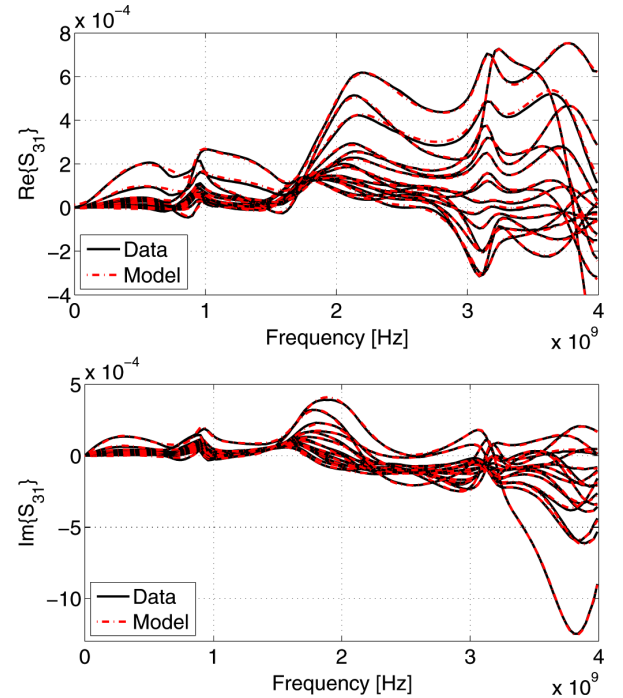


Fig. 6. Parametric model of the elementary horizontal trace of Section V-B: comparison of the  $S_{31}$  model response with the original scattering data, for several combinations of the parameters  $x_2$  and  $y_2$ . In spite of the small magnitude of the parameter, excellent fitting accuracy can be observed.

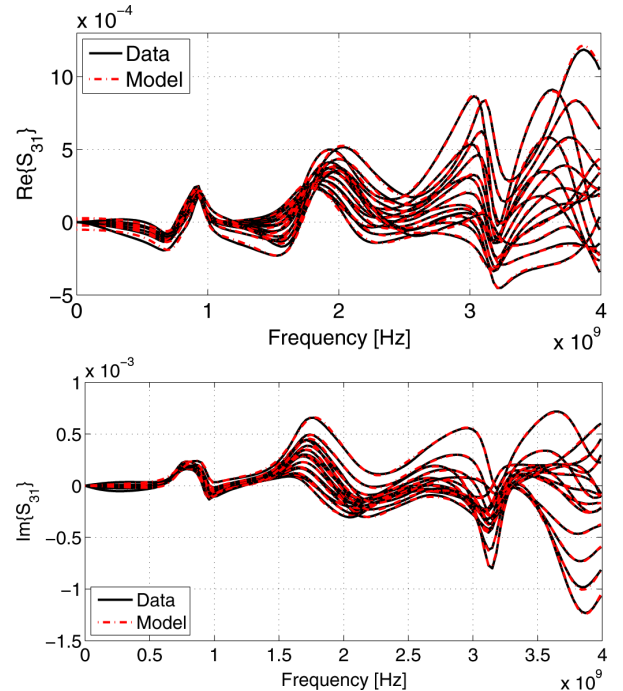


Fig. 7. As in Fig. 6, but for the case of a vertical trace.

resorts to standard vector fitting for the model generation. Both models were then cast into an equivalent circuit, and simulated in a SPICE environment. A sinusoidal ac source with 50- $\Omega$  internal impedance was connected to port 2, and a 50- $\Omega$  resistor was connected to port 3. The  $S_{21}$  scattering parameter for both models, obtained from the port voltages and currents computed

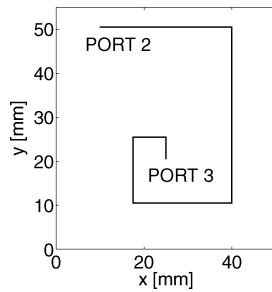


Fig. 8. Geometry of the PCB trace considered in the validation example of Section V-C.

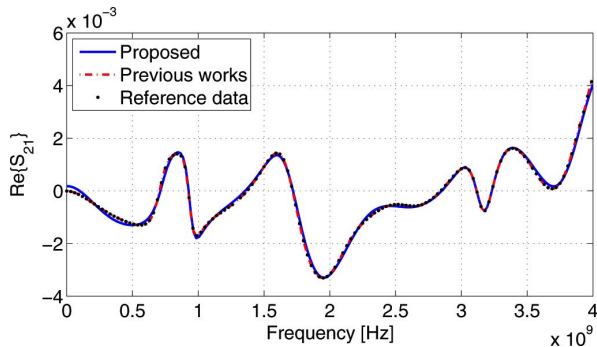


Fig. 9. Comparison of the  $S_{21}$  coefficient of the proposed model (blue solid curve) with the same coefficient of the model generated with [1] and [2] (dash-dot red curve), obtained with a SPICE ac simulation. The reference and scattering data are also depicted (black dotted curve).

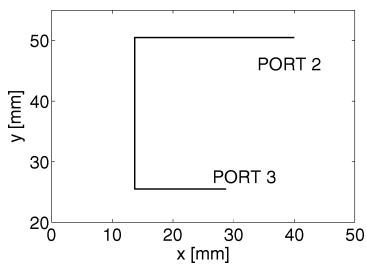


Fig. 10. Path of the microstrip considered in the application example of Section V-D.

by the simulator, is depicted in Fig. 9 versus the original scattering response (4). The very good agreement among the three curves confirms the validity of the proposed approach.

#### D. Transient Simulations

We now apply the proposed technique to predict the interference generated by the cellphone antenna on a U-shaped data link. The trace geometry is depicted in Fig. 10 together with the ports numbering. Coupling between the antenna and the trace was modeled with the strategy of Section IV-C, that delivered a stable SPICE-compatible equivalent circuit. At port 2, we connected the behavioral model [19] of a real I/O driver for mobile applications, operating at 0.6 V and driven by a 80-MHz digital signal. Port 3 was instead closed on a 1-pF capacitor represent-

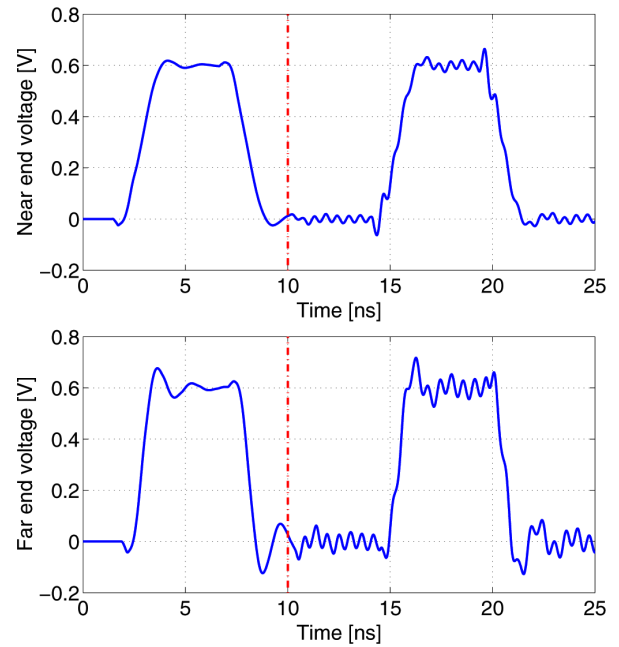


Fig. 11. (Top) Near end and (bottom) far end voltage for the cellphone interconnect described in Section V-D. The dash-dot vertical lines denote the start of antenna transmission.

ing the parasitic capacitance of the input stage of the receiving chip. In order to compare the link operation with and without the EMI, we let the antenna transmit a 1-W continuous sinusoidal wave at 1.8 GHz only 10 ns after the beginning of the transient simulation. The simulation results, obtained with a SPICE solver, are displayed in Fig. 11, and allow a precise assessment of the antenna interference under realistic operating conditions for the data link. We observe that, even if the antenna transmitted power is within the normal operation range, the digital waveform is significantly corrupted by the antenna interference, emphasizing the usefulness of the proposed models for a reliable design of interconnects in mobile devices.

## VI. CONCLUSION

We presented an efficient strategy for modeling and simulating PCB traces in mobile devices including the EMI caused by one or more transmitting antennas. The method is computationally very efficient, as it requires only one full-wave simulation to compute the generalized scattering coefficients of the whole antenna-trace system for an arbitrary trace geometry. These coefficients are then converted into an equivalent circuit model that has the unprecedented feature of being parameterized by the trace geometry. This innovation enables an on-the-fly regeneration of the equivalent circuit for a different trace geometry, and is, therefore, very appealing for sensitivity, optimization, and what-if analyses. Application to a mobile phone interconnect shows how the proposed technique enables EMI-related analyses directly within a standard circuit simulator.



## ACKNOWLEDGMENT

The first author would like to gratefully acknowledge the support provided by Istituto Superiore Mario Boella, Torino, Italy. The authors would also like to acknowledge Dr. I. Kelandar and Dr. P. Kotiranta (NOKIA) for providing the cellphone geometry used in the paper.

## REFERENCES

- [1] S. Grivet Talocia, M. Bandinu, F. Canavero, I. Kelandar, and P. Kotiranta, "Fast evaluation of electromagnetic interference between antenna and PCB traces for compact mobile devices," in *Proc. IEEE Int. Symp. Electromagn. Compat. (EMC 2008)*, 2010, pp. 1–5.
- [2] S. Grivet-Talocia, M. Bandinu, F. Canavero, I. Kelandar, and P. Kotiranta, "Fast assessment of antenna-PCB coupling in mobile devices: A macromodeling approach," in *Proc. 20th Int. Zurich Symp. Electromagn. Compat.*, 2009, pp. 193–196.
- [3] C. Paul, *Analysis of Multiconductor Transmission Lines*. New York, NY: Wiley, 1994.
- [4] C. Wei, R. Barrington, J. Mautz, and T. Sarkar, "Multiconductor transmission lines in multilayered dielectric media," *IEEE Trans. Microw. Theory Tech.*, vol. 32, no. 4, pp. 439–450, 1984.
- [5] K. Coperich, J. Morsey, V. Okhmatovski, A. Cangellaris, and A. Ruehli, "Systematic development of transmission-line models for interconnects with frequency-dependent losses," *IEEE Trans. Microw. Theory Tech.*, vol. 49, no. 10, pp. 1677–1685, Oct. 2001.
- [6] A. Agrawal, H. Price, and S. Gurbaxani, "Transient response of multiconductor transmission lines excited by a nonuniform electromagnetic field," *IEEE Trans. Electromagn. Compat.*, vol. EMC-22, no. 2, pp. 119–129, May 1980.
- [7] CST Microwave Studio. (2006). [Online]. Available: [www.cst.de](http://www.cst.de)
- [8] B. Gustavsen and A. Semlyen, "Rational approximation of frequency domain responses by vector fitting," *IEEE Trans. Power Del.*, vol. 14, no. 3, pp. 1052–1061, Jul. 1999.
- [9] P. Triverio, M. Nakhla, and S. Grivet Talocia, "Parametric macromodeling of multiport networks from tabulated data," presented at the 16th Topical Meet. Electr. Perform. Electron. Packag. (EPEP), Atlanta, GA, Oct. 29–31 2007.
- [10] P. Triverio, S. Grivet Talocia, and M. Nakhla, "An improved fitting algorithm for parametric macromodeling from tabulated data," presented at the 12th Workshop Signal Propag. Interconnects (SPI 2008), Avignon, France, May 12–15, 2008.
- [11] D. Deschrijver, T. Dhaene, and D. De Zutter, "Robust parametric macromodeling using multivariate orthonormal vector fitting," *IEEE Trans. Microw. Theory Tech.*, vol. 56, no. 7, pp. 1661–1667, Jul. 2008.
- [12] P. Triverio, S. Grivet-Talocia, and M. S. Nakhla, "A parameterized macromodeling strategy with uniform stability test," *IEEE Trans. Adv. Packag.*, vol. 32, no. 1, pp. 205–215, Feb. 2009.
- [13] D. Deschrijver and T. Dhaene, "Stability and passivity enforcement of parametric macromodels in time and frequency domain," *IEEE Trans. Microw. Theory Tech.*, vol. 56, no. 11, pp. 2435–2441, Nov. 2008.
- [14] S. Grivet-Talocia, S. Acquadro, M. Bandinu, F. Canavero, I. Kelandar, and M. Rouvala, "A parameterization scheme for lossy transmission line macromodels with application to high speed interconnects in mobile devices," *IEEE Trans. Electromagn. Compat.*, vol. 49, no. 1, pp. 18–24, Feb. 2007.
- [15] T.J. Rivlin, *Chebyshev Polynomials: From Approximation Theory to Algebra and Number Theory*, 2nd ed. New York: Wiley, 1990.
- [16] S. Grivet-Talocia and M. Bandinu, "Improving the convergence of vector fitting for equivalent circuit extraction from noisy frequency responses," *IEEE Trans. Electromagn. Compat.*, vol. 48, no. 1, pp. 104–120, Feb. 2006.
- [17] C. K. Sanathanan and J. Koerner, "Transfer function synthesis as a ratio of two complex polynomials," *IEEE Trans. Autom. Control*, vol. AC-9, no. 1, pp. 56–58, Jan. 1963.
- [18] Q. Zhang, *Neural Networks for RF and Microwave Design*. Norwood, MA: Artech House, 2000.
- [19] I. Stievano, I. Maio, and F. Canavero, "M<sub>π</sub>log, macromodeling via parametric identification of logic gates," *IEEE Trans. Adv. Packag.*, vol. 27, no. 1, pp. 15–23, Feb. 2004.



**Piero Triverio** (S'06–M'09) received the M.Sc. and Ph.D. degrees in electronics engineering from the Politecnico di Torino, Torino, Italy, in 2005 and 2009, respectively.

He was with the Computer Aided Engineering Group at Carleton University, Ottawa, Canada, during 2005 and 2007. He is currently a Research Assistant with the Electromagnetic Compatibility Group in the Department of Electronics, Politecnico di Torino. His research interests include numerical methods for signal integrity and EMC

analyses.

Dr. Triverio is a corecipient of the 2007 Best Paper Award of the IEEE TRANSACTIONS ON ADVANCED PACKAGING, the Best Paper Award presented at the IEEE 17th Topical Meeting on Electrical Performance of Electronic Packaging, in 2008, and the Best Student Paper Award at the IEEE 15th Topical Meeting on Electrical Performance of Electronic Packaging, in 2006.



**Stefano Grivet-Talocia** (M'98–SM'07) received the Laurea and Ph.D. degrees in electronic engineering from the Politecnico di Torino, Torino, Italy.

From 1994 to 1996, he was with the NASA Goddard Space Flight Center. He is currently an Associate Professor of circuit theory in the Department of Electronics, Politecnico di Torino. His research interests include passive macromodeling of lumped and distributed interconnect structures, modeling and simulation of fields, circuits, and their interaction, wavelets, time–frequency transforms, and their ap-

plications. He is the author of more than 100 journal and conference papers.

Dr. Grivet-Talocia is the corecipient of the 2007 Best Paper Award of the IEEE TRANSACTIONS ON ADVANCED PACKAGING and the IBM Shared University Research Award in 2007, 2008, and 2009. He was an Associate Editor for the IEEE TRANSACTIONS ON ELECTROMAGNETIC COMPATIBILITY from 1999 to 2001.



**Michelangelo Bandinu** received the Laurea degree in electronic engineering from the Politecnico di Torino, Torino, Italy, in 2005.

He was with IBM Deutschland Entwicklung GmbH, Boeblingen, Germany, where he was involved in the field of packaging development within the IBM Systems and Technology Group. He is currently a Research Assistant with the Electromagnetic Compatibility Group in the Department of Electronics, Politecnico di Torino. His research interests include modeling and simulation of interconnect structures,

including actual and future chip carriers, multichip and single-chip modules, cards, boards, and connectors. His research interests include modeling and macromodeling of lumped and distributed interconnects for system analysis and design under signal integrity and EMC constraints.



**Flavio G. Canavero** (M'90–SM'99–F'07) received the Laurea degree in electronic engineering from the Politecnico di Torino, Torino, Italy, in 1977, and the Ph.D. degree from the Georgia Institute of Technology, Atlanta, in 1986.

He is currently a Professor of circuit theory and electromagnetic compatibility in the Department of Electronics, Politecnico di Torino. His research interests include signal integrity and electromagnetic compatibility. He has made significant contributions to the modeling of circuit and electronic intercon-

nects. He is the author or coauthor of about 200 papers published in international journals and conference proceedings.

Dr. Canavero has been the Editor-in-Chief of the IEEE TRANSACTIONS ON ELECTROMAGNETIC COMPATIBILITY and a member of the IEEE Press Editorial Board. He has been the Chair of the International Union of Radio Science (URSI) Commission E (Noise and Interference). He is the recipient of the International Business Machines Corporation (IBM) Faculty Award for the triennium 2003–2005, the Intel Research Grant for 2008, and several Best Paper Awards and IEEE recognitions. He has been the Organizer of the Workshop on Signal Propagation on Interconnects during 2001–2003 and 2007. He is currently a member of the Scientific Steering Committees of several International Conferences in the field of electromagnetic compatibility and electrical performance of interconnects and packages. He is the Technical Editor of the IEEE EMC SOCIETY NEWSLETTER.